

# Modeling of Signal and Power Integrity in System on Package Applications

Madhavan Swaminathan and A. Ege Engin  
Packaging Research Center, School of Electrical and Computer Engineering,  
Georgia Institute of Technology, Atlanta GA

**Abstract**—We present a method for fast analysis of signal and power integrity in system-on-package applications based on a recently developed multilayered finite difference method (M-FDM). First we present a rapid solver that can be used to extract materials properties of dielectrics. The extracted frequency-dependent dielectric constant and loss tangent can then be used in any field simulator for improved accuracy. Then we present M-FDM for simulation of system-on-package applications. In order to accurately model multilayered planar structures, which are three dimensional, M-FDM combines two-dimensional models for power/ground planes using a multilayered unit cell approach. In this way, noise coupling can be considered not only in the transversal direction between two planes, but also vertically from one plane pair to another through the apertures and via holes. For a co-simulation of signal and power integrity, transmission line models also need to be included. The interaction between the signal transmission and power distribution modes is taken into account using a modal decomposition technique. An equivalent circuit model becomes available based on this finite difference approximation as well. Based on this network representation, second order effects such as fringe and gap fields can be included in M-FDM using equivalent circuit models for these fields. This results in a very accurate method that can be used for fast analysis of signal and power integrity in arbitrary package and board designs having any stack-up configuration and number of layers.

## I. INTRODUCTION

There can be many power/ground layers with via holes and cut-outs in a system-on-package as shown in Fig. 1. These planes can be a major factor for noise coupling. There can be noise coupling not only in the transversal direction between two planes, but also vertically from one plane pair to another through the apertures and via holes. In addition, noise voltage that gets coupled to the edge of the board may cause significant electromagnetic interference. Hence, accurate modeling of power/ground planes is critical to estimate the noise levels.

Excessive supply voltage fluctuations also get coupled to the transmission lines, causing signal integrity problems. For example, mode conversion at vias due to return-path discontinuities is one of the main contributors to power/ground noise in packages. At the via hole, the parallel-plate mode gets excited due to switching signal currents, and conversely,

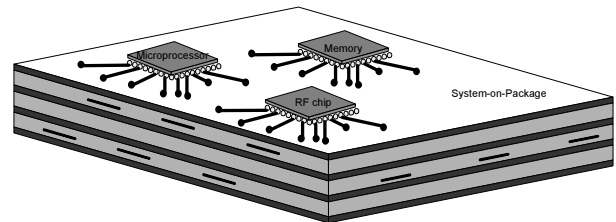


Fig. 1. Multilayered System-on-Package

the noise voltage between the planes gets coupled to the stripline mode. In order to consider this mode conversion, a modal decomposition technique can be applied [1], [2], [3], [4], [5], [6]. In these approaches, the transmission lines and power/ground planes can be modeled separately and combined together using controlled sources.

Finite-difference frequency domain (FDFD) solution of the Helmholtz equation has been recently proposed as a simple and efficient method for the modeling of single plane pairs [7] and has been extended to multiple plane pairs as the multilayered finite-difference method (M-FDM) [8]. M-FDM has been extended to incorporate transmission lines as well, based on the modal decomposition method [9].

Package structures typically contain split planes and power islands. The coupling between them is neglected in this formulation. Also, any narrow width lines present in the structure will be modeled inaccurately. In the case of narrow-width lines, the effect of fringing fields must be modeled. For the case of slots in the plane, gap coupling has to be modeled. These second-order effects have been recently included in M-FDM using equivalent circuit models [10].

In this paper we show the fundamentals of M-FDM and how it is capable of modeling 3D structures using a proper combination of 1D and 2D models as well as parasitic fringe and gap fields. This provides overall a very general method, which can represent the vertical and horizontal coupling in a multilayered structure including signal lines and power/ground planes. As a result, accurate modeling of a full system-on-package or PCB becomes possible.

## II. VERTICAL COUPLING THROUGH MULTILAYERED PLANES

In a single plane pair, the fundamental noise coupling occurs in the horizontal direction between the two planes that constitute the plane pair. The plane pair acts essentially as a cavity resonator. In a multilayered structure, there can be noise coupling in both the horizontal and vertical directions through the power/ground planes. Such a structure consists of multiple plane pairs. The vertical coupling can then be considered as a coupling between these plane pairs. Assuming a well developed skin effect, the vertical coupling through the conductors can be neglected. The major vertical coupling occurs through the interactions between these plane pairs at their boundaries. This coupling mechanism can be described as the aperture coupling or the coupling due to the wrap-around currents as described in the following example.

Fig. 2(a) shows a simple one-dimensional case, where the right half of the middle plane is missing. For this example, there are three plane pairs based on different combinations of the planes. Assume that there is a current on the middle plane with its return current on the bottom plane. These currents are confined inside the plane pair 2 as shown in the figure. When this current arrives the right boundary of this plane pair, it can wrap-around the aperture. Hence this so-called wrap-around current can excite currents in plane pair 1 and plane pair 3 as shown in the figure. This is a direct current coupling path between the plane pairs and is critical for accurate estimation of coupling in multilayered planes.

In order to model the wrap-around currents, the three plane pairs can be modeled separately and interconnected with each other as shown in Fig. 2(b). Such an interconnection enforces the correct boundary conditions such that the wrap-around currents are taken into account as shown in the figure. Note that the electric field is assumed to have no horizontal components. As a result of this, the fringe and gap fields are neglected. Such an assumption is accurate for large structures separated with a dielectric that has a small thickness. Such second order effects can be taken into account using additional circuit elements as it will be shown in the following sections.

Regarding a practical implementation of the modeling approach shown in Fig. 2(b), several points need consideration. First of all, there should be no conflict between the models regarding a common reference terminal for the definition of voltages at the interconnection. This point becomes important if circuit models with different ground references are being used to model the plane pairs. Another problem is locating the boundaries between the plane pairs and realizing the interconnections. This can be very difficult for a structure having many number of layers that have complicated boundaries.

The multilayered finite-difference method (M-FDM) that is presented in this paper overcomes these practical problems by defining multilayered unit cell models that have the same ground reference, such that interconnection of the unit cells becomes straightforward. The following section explains the details of M-FDM.

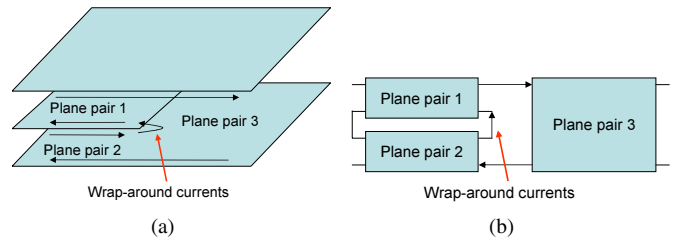


Fig. 2. Wrap-around currents due to the coupling through a gap in the middle plane for a simple one-dimensional case. (a) Geometry. (b) Equivalent network model.

## III. MATERIALS CHARACTERIZATION USING A RAPID SOLVER

The underlying elliptic partial differential equation for the modeling of planes is a Helmholtz equation

$$(\nabla_T^2 + k^2)u = -j\omega\mu dJ_z, \quad (1)$$

where  $\nabla_T^2$  is the transverse Laplace operator parallel to the planar structures,  $k$  is the wave number,  $u$  is the voltage,  $\omega$  is the angular frequency,  $\mu$  is the permeability,  $d$  is the distance between the planes, and  $J_z$  is the current density injected normally to the planes [11]. The problem definition is completed by assigning homogenous Neumann boundary conditions, which correspond to assuming a magnetic wall, or an open circuit, on the periphery of the planes.

One method to solve the Helmholtz equation is by applying the finite-difference scheme. The 2-dimensional Laplace operator (1) can be approximated as

$$\nabla_T^2 u_{i,j} = (u_{i,j-1} + u_{i,j+1} + u_{i-1,j} + u_{i+1,j} - 4u_{i,j})/h^2 \quad (2)$$

within an error in the order of  $O(h^2)$ , where  $h$  is the mesh length and  $u_{i,j}$  is the voltage at node  $(i, j)$  for the cell-centered discretization.

Applying this 5-point approximation on the Helmholtz equation yields

$$u_{i,j-1} + u_{i,j+1} + u_{i-1,j} + u_{i+1,j} - 4u_{i,j} + h^2 k^2 u_{i,j} = -h^2 j\omega\mu dJ_z, \quad (3)$$

which gives a system of linear equations when applied to all nodes on the plane.

Obtaining the frequency response of a plane pair requires the solution of a large sparse linear system that is obtained by applying (3) on all nodes on the plane and considering the boundary conditions. For the general case of a plane pair with an arbitrary shape, this involves the solution of a linear equation system [8]. For solid rectangular planes, however, this solution can be obtained using a "rapid" method based on the Fourier transform [12].

Applying the discrete cosine transform to (3) yields

$$\hat{u}_{m,n} = \frac{-h^2 j\omega\mu d \hat{J}_z}{(2 \cos \frac{\pi m}{J} + 2 \cos \frac{\pi n}{J} - 4 + h^2 k^2)}, \quad (4)$$

where  $\hat{u}_{m,n}$  is the discrete cosine transform of  $u_{i,j}$ . Hence the procedure for solving the Helmholtz equation for rectangular

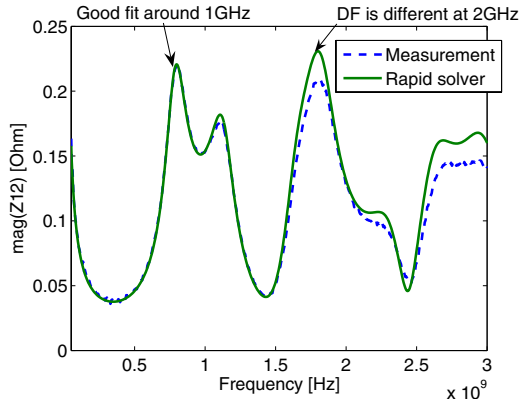


Fig. 3. Comparison between the rapid solver and measurement results (dielectric constant (DK)=27.6 at 1GHz, loss tangent (DF)=0.03)

planes using the discrete cosine transform can be summarized as:

- Compute the discrete cosine transform of the right hand side ( $-h^2 j\omega\mu d \hat{J}_z$ ).
- Compute  $\hat{u}_{m,n}$  from (4).
- Inverse transform  $\hat{u}_{m,n}$  to obtain the solution  $u_{i,j}$ .

The discrete cosine transform ensures that homogeneous Neumann boundary conditions (i.e., open circuit boundary conditions) hold at the boundaries. This rapid solution method does not require the solution of a linear equation system. Hence it provides a very efficient way of analyzing solid rectangular planes. As an example, more than a 50X speed-up in simulation time could be obtained using the rapid solver compared to the conventional solution using a sparse matrix solver for a 500x500 discretization.

Since power/ground planes in a system-on-package contain via holes and cut-outs, the rapid solver is not suitable for analyzing such structures. An equivalent-circuit based model can be applied in this case, as it will be shown in the next section. However, the rapid solver can be quite useful to extract the materials properties of dielectrics [13], where a continuous rectangular plane pair is used as a resonator. By matching the simulation results to the measurement results, the frequency-dependent dielectric constant and loss tangent can be extracted. Such a method relies on a lot of simulations with different materials properties, hence the rapid solver can speed-up this process significantly.

To illustrate the application of the rapid solver for materials characterization, a parallel-plate capacitor, which has dimensions of 33.3mm x 33.3mm, was measured. The 2-port Z-parameters of the structure was obtained by placing the ports on two opposite corners on the planes. Transfer impedance (Z12) was used for comparison with measurements, since it is not affected by the probe inductance and resistance.

Fig. 3 shows the comparison between the rapid solver and the magnitude of measured Z12, where the dielectric properties were specified as  $\epsilon_r = 27.6$  at 1GHz and  $\tan \delta = 0.03$  to the rapid solver. It can be seen that at around 1GHz, the rapid solver matches excellently with the measurements. At higher

frequencies, there is more attenuation in the measurements. Hence, the loss tangent seems to be increasing with frequency, and another fit is required around that frequency. In this way, the materials properties can be extracted for all resonance frequencies of the structure.

#### IV. MULTILAYERED FINITE DIFFERENCE METHOD (M-FDM)

##### A. Single Plane Pairs

The rapid solver cannot be used for planes with arbitrary structures. Models for such structures can be obtained by an interconnection of unit cells based on the finite difference approximation. Via holes or cut-outs in the planes can then be taken into account by removing the unit cells at those locations. There are also several unit cell types as shown in Fig. 4. Note that the impedances shown in the unit-cells are half of the total impedances between two neighboring nodes. When unit cells are connected with each other, two half impedances from neighboring unit cells establish the correct impedance value. The T-unit cell model is based on a 5-point approximation of (1), whereas the X-unit cell model can be obtained from the 9-point finite-difference formula. The T-unit cell results in the well-known bedspring model for a plane consisting of inductors ( $L$ ) between neighboring nodes, and capacitors ( $C$ ) from each node to ground. In the figure, the per unit cell impedance and admittance are represented as

$$Z = R + j\omega L \quad (5)$$

and

$$Y = G + j\omega C, \quad (6)$$

where the per unit cell parameters can be obtained as

$$C = \frac{\epsilon h^2}{d} \quad (7)$$

$$L = \mu d \quad (8)$$

$$R = \frac{2}{\sigma t} + 2\sqrt{\frac{j\omega\mu}{\sigma}} \quad (9)$$

$$G = \omega C \tan \delta, \quad (10)$$

for a given permittivity  $\epsilon$ , permeability  $\mu$ , conductivity  $\sigma$ , conductor thickness  $t$ , loss tangent  $\tan \delta$ , and cell size  $h$ . The dielectric constant and loss tangent are in general frequency dependent as discussed in the previous section. Note that  $R$  in (9) represents the internal impedance, including both the dc and the skin effect resistance, as well as the contribution of the internal inductance.

The main difference of the X-unit cell is that it includes a direct inductive path to the diagonally neighboring cells in addition to the neighboring cells sharing a side. However, both T- and X-models are second order approximations to the Helmholtz equation. As a result of this, the improvement in accuracy using the new X-unit cell is not significant [14]. Since the well-known T-unit cell based on the 5-point discretization results in a simpler model, it is going to be used in the following sections.

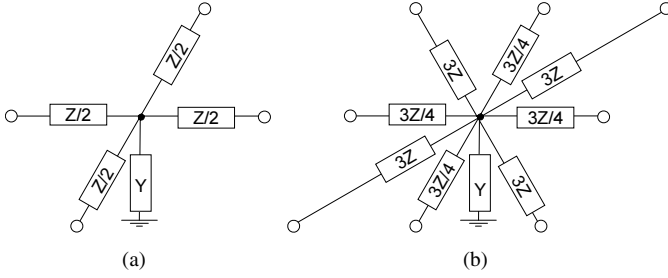


Fig. 4. Unit-cell models for a single plane pair. (a) T-unit cell. (b) X-unit cell.

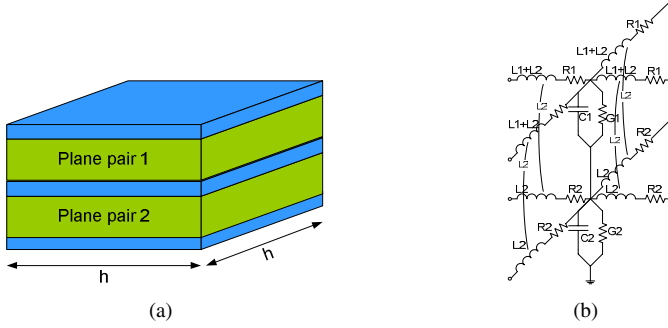


Fig. 5. (a) Geometry and (b) combined T-unit cell model for multilayered planes (for the example of three planes).

### B. Multilayered Planes

The unit cell models shown in Fig. 4 use a common ground node. In a multilayered structure consisting of more than two planes, unit cells of different plane pairs can assign this ground potential to different planes. Therefore, such unit cells cannot be stacked on top of each other without any modification to model a multilayered plane, since each unit-cell is modeled by a grounded  $n$ -port. A straightforward stacking would short-circuit the elements between two ground connections, resulting in a completely wrong model. As a result, a multilayered unit-cell model becomes necessary. Such a model can be obtained using the indefinite admittance matrices of individual unit cell models [8]. For example, Fig. 5 shows an equivalent circuit model for a sample unit cell including three planes, where the bottom plane is chosen as the common reference terminal. The per unit cell parameters do not always have to be defined between two adjacent planes. For example, a unit cell can include inductances and capacitance between distant planes, if there are slots on the planes between them. The total nodal admittance matrix can be constructed easily by interconnecting the resulting unit cells with each other.

### C. Fringe and Gap Fields

The formulation discussed in the previous section assumes that each unit cell sees a plane-pair of infinite extent along the lateral directions. The formulae used to calculate the capacitor and inductor elements (7)-(10) are essentially parallel plate formulae. However, fringing fields occur at edge discontinuities. This implies that both the per-unit-length (pul)

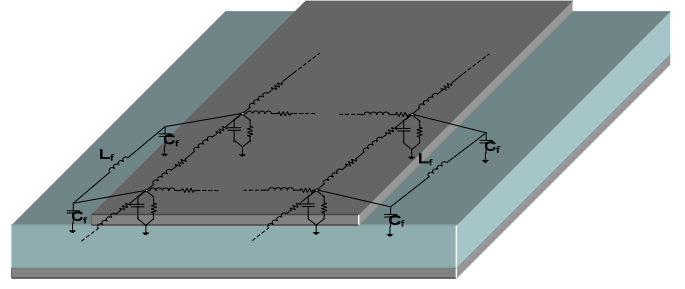


Fig. 6. M-FDM including fringe elements

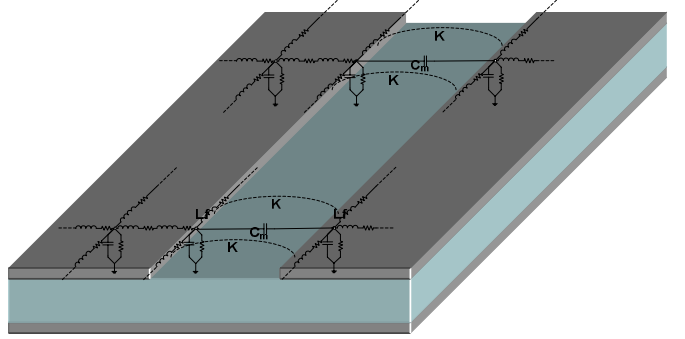


Fig. 7. M-FDM including gap elements

inductance and capacitance will be different from that obtained from parallel plate formulae. To compensate for this fringe effect, additional capacitors and inductors are added around the edges of the planes as shown in Fig. 6.

The gap effect leads to coupling between physically separated metal patches when the distance of separation between them approaches the dielectric thickness. The coupling can be especially significant when the patches resonate. Fig. 7 shows two patches separated by a gap. The requirements for the model are that it should be a lumped network that couples only the nodes on either side of the slot. The E-field coupling is represented by a capacitor,  $C_m$ , connected between the nodes that lie across the gap. The H-field coupling is modeled by a mutual coupling factor,  $K$ , as shown in the figure.

The values of the circuit elements for both the fringe and gap fields can be extracted using closed-form equations [10].

### D. Transmission Lines

Striplines are embedded transmission lines between two planes as shown in Fig. 8(a). Based on modal decomposition [15], such a stripline can be added into the model of a multiple plane structure as shown in Fig. 8(b), where the coupling coefficient can be found as

$$k = -\frac{h1}{h1 + h2}. \quad (11)$$

A microstrip line can be regarded as just a special case of a stripline, where  $k = 0$  or  $k = -1$  in (11) depending on whether it is referenced to the voltage reference plane or not.

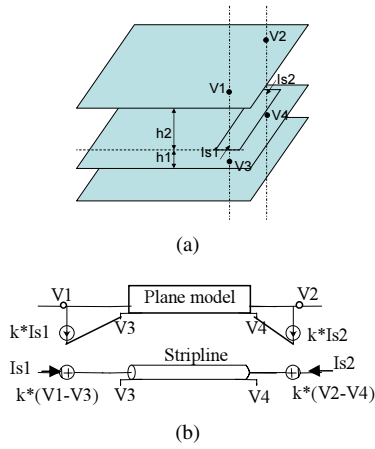


Fig. 8. (a) Geometry and, (b) model for a stripline in a multilayered planar structure

## V. NUMERICAL RESULTS

The simulated test case is a mixed signal board with split planes separating the digital module with an FPGA and an RF transceiver module. The board layout is shown in Fig. 9(a). Ports 1 and 2 are placed at the location of the FPGA and the RF transceiver respectively. Noise generated by the FPGA can couple through the PDN and cause degradation in the performance of the RF module. From the insertion loss result shown in Fig. 9(b), it can be seen that significant coupling occurs at 2.1, 2.8, 3.5 and 5 GHz. Also, it can be seen that the results from M-FDM and Sonnet are well correlated. The time per frequency sample for M-FDM was 3s as compared to 340s for Sonnet, which represents a speed up of 113X.

## VI. CONCLUSION

This paper presented the multilayered finite-difference method (M-FDM), which can be used for signal and power integrity analysis of system-on-package applications. M-FDM extends the standard approach of solving the 2D Helmholtz equation for power/ground planes to multilayered planar structures. The accuracy is improved by taking into account the frequency-dependent behavior of materials properties (that are obtained using a rapid solver) as well as by considering fringe and gap fields. For a full signal integrity analysis, the transmission lines are incorporated using the modal decomposition technique. As a result, frequency responses of multilayered packages and boards can be obtained efficiently with accuracy approaching full-wave solvers.

## REFERENCES

- [1] J. Fang, Y. Chen, Z. Wu, and D. Xue, "Model of interaction between signal vias and metal planes in electronics packaging," in *Proc. Electrical Performance of Electronic Packaging*, 1994, pp. 211–214.
- [2] H. Liaw and H. Merkelo, "Simulation and modeling of mode conversion at vias in multilayer interconnections," in *Proc. Electronic Components and Technology Conference*, 1995, pp. 361–367.
- [3] R. Abhari, G. V. Eleftheriades, and E. van Deventer-Perkins, "Physics-based CAD models for the analysis of vias in parallel-plate environments," *IEEE Trans. Microwave Theory Tech.*, vol. 49, pp. 1697–1707, Oct. 2001.

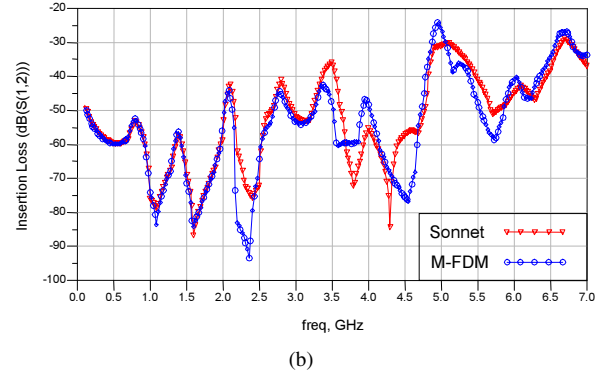
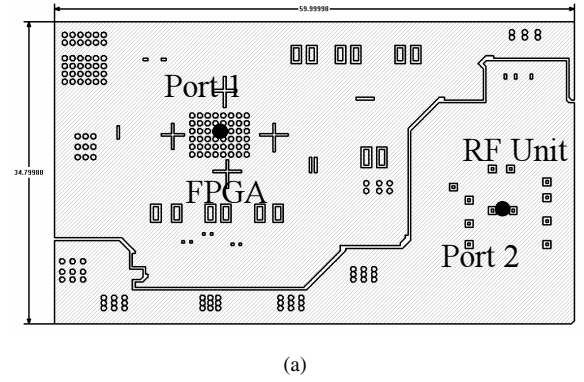


Fig. 9. Mixed-signal board. (a) Geometry. (b) Simulation results.

- [4] S. Chun, L. Smith, R. Anderson, and M. Swaminathan, "Model to hardware correlation for power distribution induced I/O noise in a functioning computer system," in *Proc. Electronic Components and Technology Conference*, May 2002, pp. 319–324.
- [5] N. Orhanovic, D. Divekar, and N. Matsui, "Structure decomposition for hybrid analysis of multilayer interconnect systems," in *Proc. Electrical Performance of Electronic Packaging*, Oct. 2002, pp. 137–140.
- [6] D. Chung, T. H. Kim, C. Ryu, E. Engin, M. Swaminathan, and J. Kim, "Effect of EBG structures for reducing noise in multi-layer PCBs for digital systems," in *Proc. Electrical Performance of Electronic Packaging*, Scottsdale, AZ, Oct. 2006, pp. 253–256.
- [7] O. Ramahi, V. Subramanian, and B. Archambeault, "A simple finite-difference frequency-domain (FDFD) algorithm for analysis of switching noise in printed circuit boards and packages," *IEEE Trans. Adv. Packag.*, vol. 26, no. 2, pp. 191–198, May 2003.
- [8] A. E. Engin, K. Bharath, M. Swaminathan, M. Cases, B. Mutnury, N. Pham, D. N. de Araujo, and E. Matoglu, "Finite-difference modeling of noise coupling between power/ground planes in multilayered packages and boards," in *Proc. Electronic Components and Technology Conference*, May 2006.
- [9] A. E. Engin, K. Bharath, K. Srinivasan, and M. Swaminatha, "Modeling of multilayered packages and boards using modal decomposition and finite difference methods," in *IEEE International Symposium on Electromagnetic Compatibility*, Portland, OR, Aug. 2006.
- [10] K. Bharath, E. Engin, M. Swaminathan, K. Uriu, and T. Yamada, "Efficient modeling of package power delivery networks with fringing fields and gap coupling in mixed signal systems," in *Proc. Electrical Performance of Electronic Packaging*, Scottsdale, AZ, Oct. 2006, pp. 59–62.
- [11] T. Itoh, Ed., *Numerical Techniques for Microwave and Millimeter-Wave Passive Structures*. John Wiley & Sons, 1989.
- [12] W. H. Press, S. A. Teukolsky, W. T. Vetterling, and B. P. Flannery, *Numerical recipes in C : the art of scientific computing - 2nd ed.* Cambridge University Press, 2002.
- [13] A. E. Engin, A. Tambawala, M. Swaminathan, S. Bhattacharya, P. Pramanik, and K. Yamazaki, "Dielectric constant and loss tangent characterization of thin high-K dielectrics using corner-to-corner plane probing,"

in *Proc. Electrical Performance of Electronic Packaging*, Scottsdale, AZ, Oct. 2006, pp. 29–32.

- [14] A. E. Engin, M. Swaminathan, and Y. Toyota, “Finite difference modeling of multiple planes in packages,” in *International Zurich Symposium on Electromagnetic Compatibility*, Feb. 2006.
- [15] A. E. Engin, W. John, G. Sommer, W. Mathis, and H. Reichl, “Modeling of striplines between a power and a ground plane,” *IEEE Trans. Adv. Packag.*, vol. 29, no. 3, pp. 415–426, Aug. 2006.